

Supporting Information

Self-Supported $\text{Co}_3\text{O}_4@\text{Zn}-\text{CoNi}_2\text{S}_4/\text{NF}$ Core-Shell Nanoarrays as an Efficient Bifunctional Electrode for Overall Water Splitting

Xuan Zhao¹, Yu Dong¹, Zhijie Wang¹, Yusheng Qiu¹, Ende Wang², Naikun Sun¹ ^{*}, Yongli Tong¹ ^{*}

Supplementary Figures and Tables

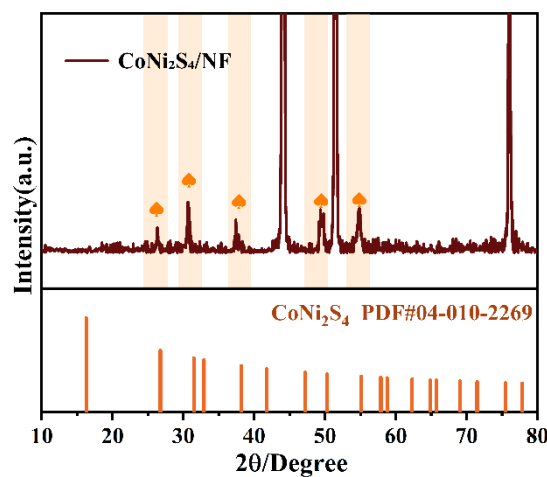


Fig S1. XRD pattern of the $\text{CoNi}_2\text{S}_4/\text{NF}$.

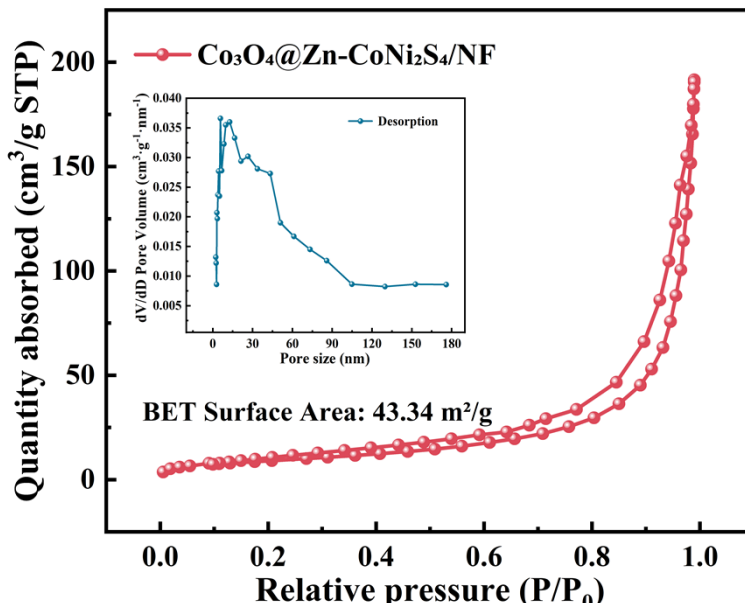


Fig.S2. N_2 adsorption-desorption isotherms and pore size distribution of $\text{Co}_3\text{O}_4@\text{Zn}-\text{CoNi}_2\text{S}_4/\text{NF}$.

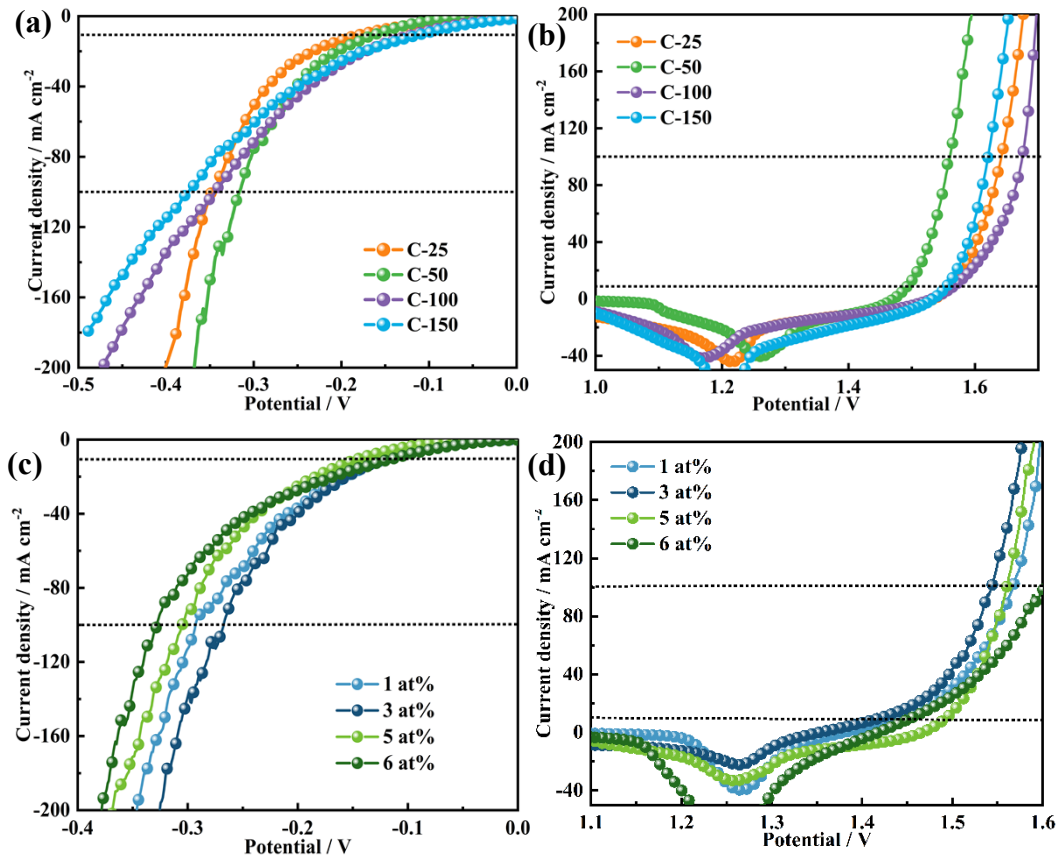


Fig. S3 (a) HER and (b) OER LSV curves of the C-25, C-50, C-100, and C-150. (c) HER and (d) OER LSV curves with varying Zn doping contents.

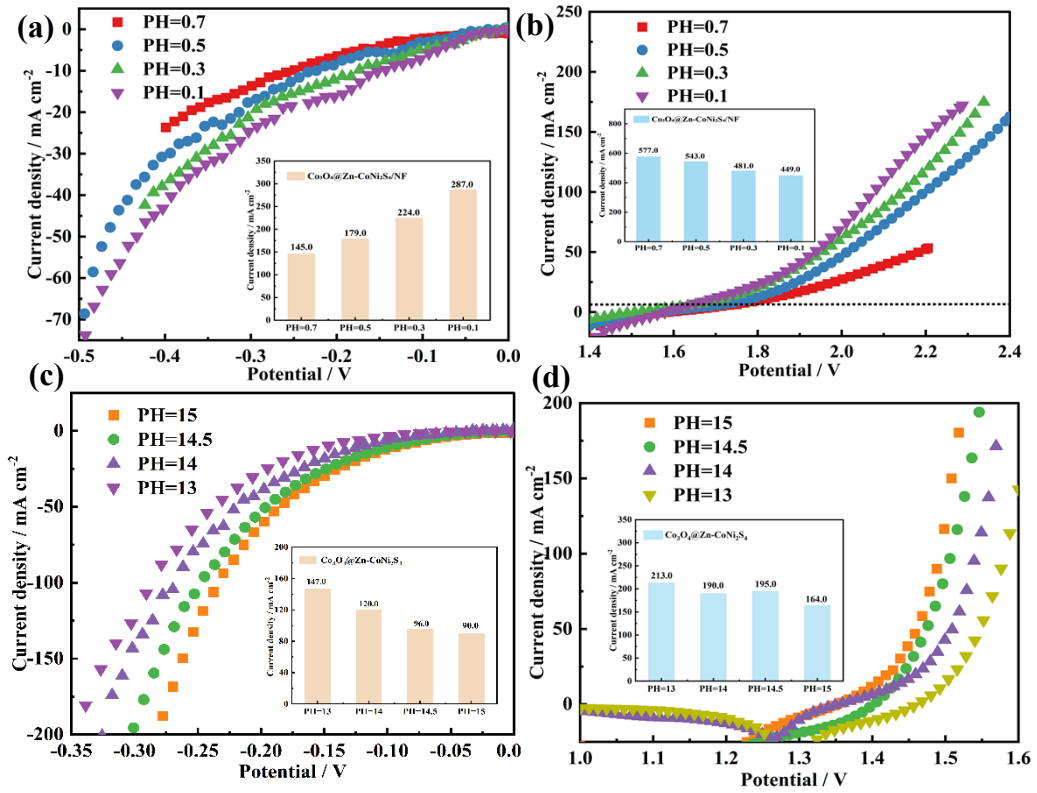


Fig. S4. LSV curves of $\text{Co}_3\text{O}_4@Zn\text{-CoNi}_2\text{S}_4$ for (a) HER and (b) OER measured in H_2SO_4 solutions ($\text{pH} \approx 0.7, 0.5, 0.3$, and 0.0) ; (c) HER and (d) OER measured in KOH solutions ($\text{pH} \approx 13.0, 14.0, 14.5$, and ~ 15.0).

In response to these comments, LSV measurements are conducted in both acidic and alkaline electrolytes to evaluate the catalytic activity of $\text{Co}_3\text{O}_4@Zn\text{-CoNi}_2\text{S}_4$. For the acidic tests, 0.1 M , 0.3 M , 0.5 M and 1.0 M H_2SO_4 are employed, corresponding to a pH range of approximately $0.7\text{--}0.0$. For the alkaline tests, 0.1 M , 1.0 M , 3.0 M and 5.0 M KOH are used, with a pH range of about $13.0\text{--}15.0$.

Given that NF undergoes corrosion in acidic electrolytes, $\text{Co}_3\text{O}_4@Zn\text{-CoNi}_2\text{S}_4$ powder is uniformly coated onto carbon cloth using a mixture of Nafion and ethanol as the binder. Electrochemical performance tests are then carried out under the same conditions as those described in the main text. The results demonstrate that the catalyst exhibits excellent catalytic activity in alkaline media, which is consistent with the main conclusions of this paper. However, its performance decreases significantly in acidic electrolytes, as illustrated in Fig. S4 (a-d) (page 3 of the Supporting Information).

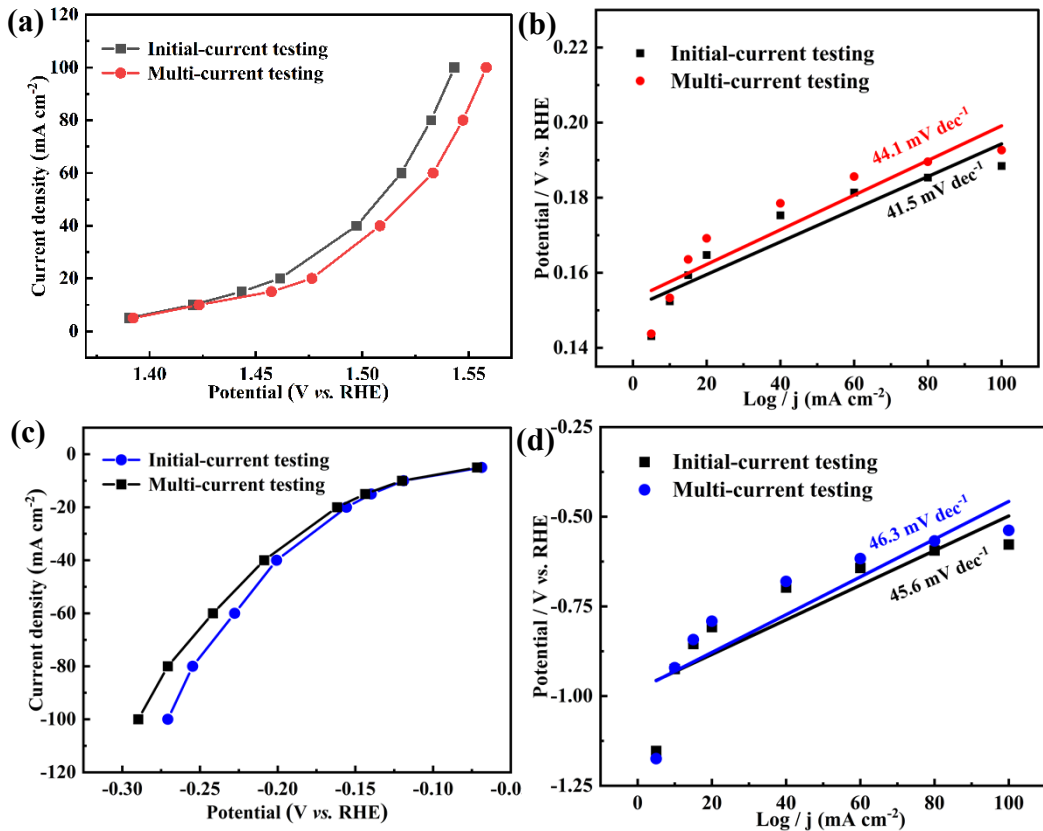


Fig. S5. Comparison of polarization curves and corresponding Tafel plots obtained from LSV and steady-state potentiostatic measurements for $\text{Co}_3\text{O}_4@\text{Zn-CoNi}_2\text{S}_4/\text{NF}$.

Table 1 The OER overpotentials and standard deviations

| Sample | η @ 10 mA cm ⁻² (V) | Standard Deviation | Sample Size |
|--|-------------------------------------|--------------------|-------------|
| $\text{Co}_3\text{O}_4@\text{Zn-CoNi}_2\text{S}_4/\text{NF}$ | 195mV | ± 2.63 | 3 |
| $\text{Co}_3\text{O}_4@\text{CoNi}_2\text{S}_4/\text{NF}$ | 265mV | ± 2.71 | 3 |
| $\text{Co}_3\text{O}_4/\text{NF}$ | 303mV | ± 2.94 | 3 |

Table 2 The HER overpotentials and standard deviations

| Sample | η @ 10 mA cm ⁻² (V) | Standard Deviation | Sample Size |
|--|-------------------------------------|--------------------|-------------|
| $\text{Co}_3\text{O}_4@\text{Zn-CoNi}_2\text{S}_4/\text{NF}$ | 120mV | ± 2.64 | 3 |
| $\text{Co}_3\text{O}_4@\text{CoNi}_2\text{S}_4/\text{NF}$ | 160mV | ± 3.25 | 3 |
| $\text{Co}_3\text{O}_4/\text{NF}$ | 168mV | ± 2.29 | 3 |

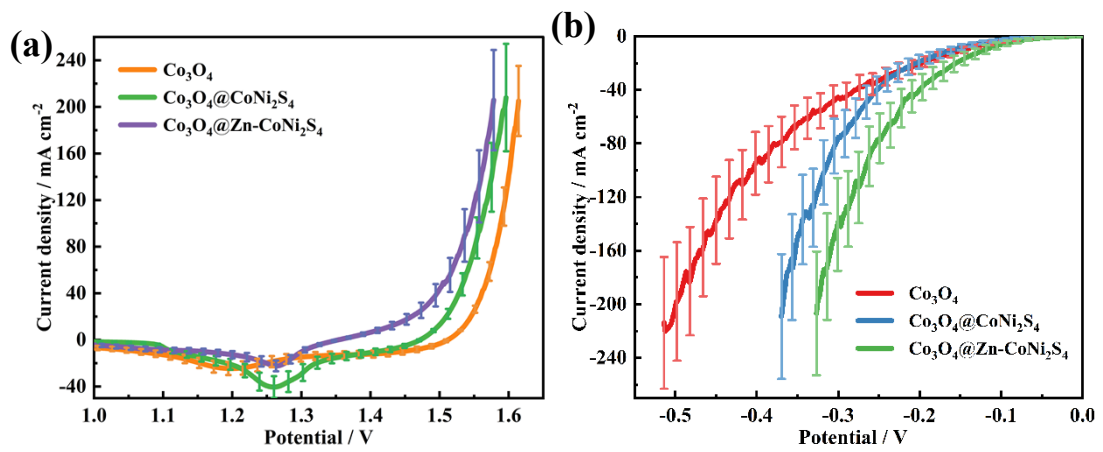


Fig. S6 Overpotential comparison at a current density of 10 mA cm^{-2} for (a) the OER and (b) the HER of $\text{Co}_3\text{O}_4@\text{Zn-CoNi}_2\text{S}_4/\text{NF}$.



Fig. S7 Schematic diagram of the faradaic efficiency measurement setup

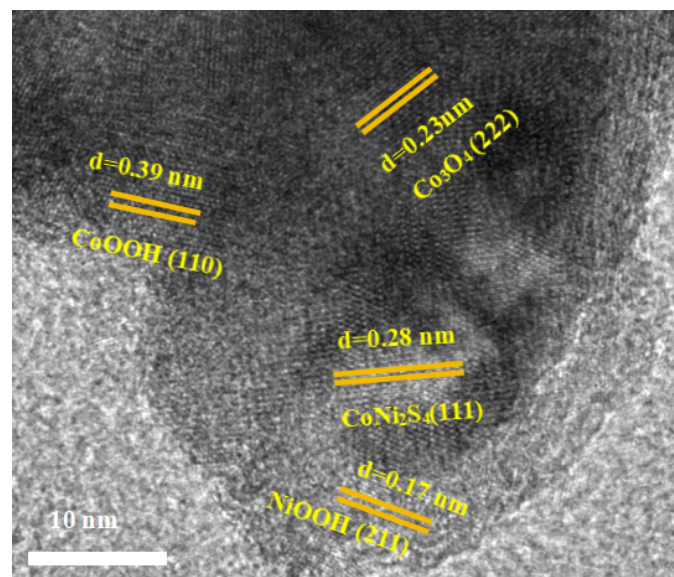


Fig. S8 HRTEM image of $\text{Co}_3\text{O}_4@\text{Zn-CoNi}_2\text{S}_4/\text{NF}$ after cycling.

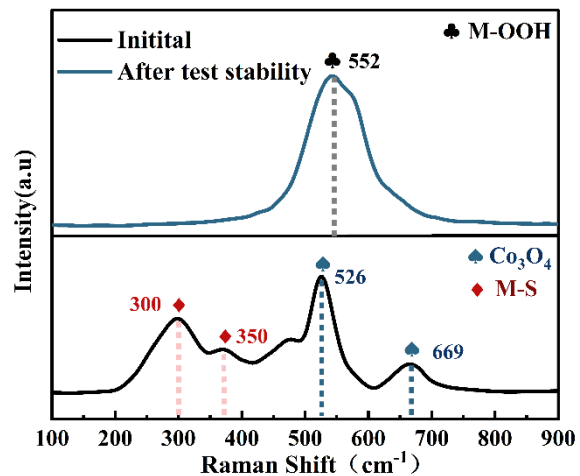


Fig. S9 Raman spectra of $\text{Co}_3\text{O}_4@\text{Zn-CoNi}_2\text{S}_4/\text{NF}$ before and after cycling.